

material properties and valve geometry) and extrinsic forces (e.g. due to blood viscosity and external forces).

Input parameters included pressures and flow values during early diastolic ventricular filling, aortic and mitral valve geometries, and blood density and viscosity values. The pig model has now been improved to use velocity waveforms as model inputs. We call this model a velocity driven model.

Measurement of left ventricular pressure (LVP), left aortic pressure (LAP), left ventricular volume and pulmonary venous flow was performed in 12 subsequent, *in vivo*, canine trials. LAP and LVP waveforms were obtained from empirical data, which was collected over a ten second period. Mean LAP and LVP waveforms were calculated from the empirical data.

An important feature of the model is that some model parameters may be used either as input data; or can be predicted as output parameters by considering the problem an inverse problem. In an inverse problem some model parameters are obtained from empirical data.

Although atrial or ventricular compliance constants cannot easily be measured directly, they may be obtained as outputs from the model, by iteratively varying the compliance values in the simulation, until simulation pressure curves match the experimentally collected data.

**Results**

Figure 1 shows results from a typical canine trial. The left hand column shows observed versus simulated results using the previously validated model. The right hand column compares the velocity driven model results. The following mean (SD) values were obtained for the respective parameter in 12 dogs:

- Aortic Compliance Constant = .181 (.21) ml<sup>-1</sup>
- Ventricular Compliance Constant = .075 (.078) ml<sup>-1</sup>
- Maximum effective valve area = 4.14 (3.45) cm<sup>2</sup>
- Stroke volume = 16.2 (6.8) ml
- Valve natural frequency = 2.65 (4.18) s<sup>-1</sup>

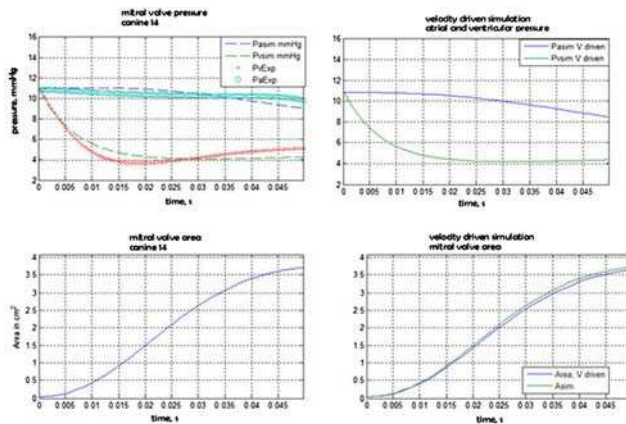


**Fig. 1** Results for the canine trial 14 (HTX-09). The upper left figure shows the simulated left atrial and ventricular pressures (dashed lines) and the experimentally measured left ventricular pressure (red Xs) and left atrial pressure (blue circles). The figure at the upper right shows the simulated pressure from the velocity driven model. The bottom left diagram shows the simulated mitral valve area in the previous model and the figure at right shows the mitral valve area generated by the velocity driven model. The left hand column shows observed versus simulated results using the previously validated model. The right hand column compares the velocity driven model results

**Conclusion**

The model uses the inverse problem method to estimate several parameters that are not easily measurable, like the natural frequency of the valve and the atrial and ventricular compliance. Because there are many non-linear parameters involved, there may not be a unique solution to the inverse problem in every case, but because the problem is sufficiently well behaved, the computer model successfully estimated the values.

In summary, the velocity driven model, using velocity waveform inputs, was able to estimate values for key parameters that were consistent with those reported in the literature. We believe this is a key step in the direction toward developing a clinically useful model for human diagnostic purposes.

**Acknowledgment**

Thanks to the German and American Fulbright Commissions for their support of Dr. Waite as a Fulbright Senior Scholar.

**A MRI study of relative organ position in the upper abdomen for changes in patient orientation: application to image-registered endoscopic ultrasound**

San José Estépar R.<sup>1</sup>, Madore B.<sup>1</sup>, Yarmarkovich M.<sup>2</sup>, Vosburgh K.G.<sup>1,2</sup>

<sup>1</sup>Brigham and Women’s Hospital, Radiology, Boston, MA, USA  
<sup>2</sup>CIMIT, Boston, MA, USA

**Keywords** Patient pose · Organ motion · Endoscopy · Laparoscopy  
**Purpose**

This paper presents a study of abdominal organ shift due to changes in body posture. A previous study [1] has reported a noticeable qualitative shift for abdominal structures, comparing prone and supine CT studies. Such measurements are relevant for the use of preoperative imaging in guiding endoscopic interventions. CT and MRI images of the torso are conventionally made with the patient supine, and this protocol is unlikely to change in conventional practice. While abdominal surgeons generally perform procedures with their patients supine, gastroenterologists use a variety of patient poses, depending on the examination. Thus the CT images made of a surgical patient will “fit” the relative organ positions observed by the surgeon in the OR, but these images will be less accurate in the endoscopy suite. Two specific examples are the conventional setting for gastroscopic studies, whether conventional or ultrasound, for which the patient is typically placed in the left lateral decubitus position, and endoscopic retrograde cholangio-pancreatography (ERCP), in which the patient is prone. Compared with their positions when the patient is supine, soft tissue structures such as the liver, the kidney (and most likely, the pancreas) will deform due to the changes in gravity and external body forces.

We have carried out a MRI study with two subjects to assess the amount of motion with respect to the supine position for the liver and the left and right kidney. Since the pancreas is tied to relatively rigid structures in the retroperitoneum, we expect this effect to be smaller than with the liver, with the movement of the kidneys and the gall bladder being in-between.

**Background**

The increasing use and quality of radiologic techniques (CT, MRI, SPECT, PET) for screening and diagnosis will stimulate the demand for minimally invasive biopsy and intervention. While these procedures might optimally be conducted inside the imaging device itself, practical considerations, including convenience and cost, will continue to limit “in scanner” approaches. Thus endoscopic and (to some extent) laparoscopic imaging are likely to be more broadly applied to the follow-up diagnosis of disease and the staging of care. As well, optical biopsy techniques, which can use smaller probes, may be increasingly utilized.

One approach to improving the guidance of instruments in real time is the use of intra-procedure ultrasound. While ultrasonic

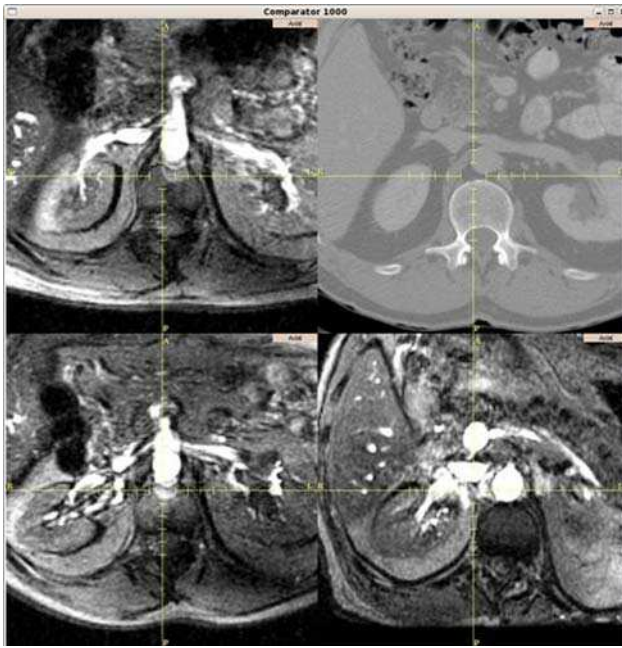


**Fig. 1** Comparison between different body postures after rigid image-based mutual information registration. Top row: MRI supine (left), CT supine (right). Bottom row: MRI prone (left), MRI right decubitus (right)

laparoscopic and endoscopic devices are widely available, they have been not maximally adopted by gastroenterologists and surgeons due to the long learning curve and lack of confidence in ultrasound interpretation, which manifests as difficulty in navigation and targeting the probe to reach the radiologically determined target. Image Registration (IR) techniques have therefore been developed; these show the position and orientation of the ultrasound probe in anatomic context and display re-formatted CT (or MR) reference images to

improve the accuracy and confidence of physician operators. The IR approach is based on two assumptions: (1) the operator may function most effectively when presented with a simplified representation of the anatomy showing only key structures to guide probe positioning, and (2) real time display of the position and orientation in this anatomic context may be more efficient than the use of more complex 3D plane displays of the radiologic information. That is, Image Registration techniques may have added value because the instrument position and orientation is displayed accessibly and understood easily and intuitively.

Experimental studies in porcine models have shown that both laparoscopic ultrasound (LUS) and endoscopic ultrasound (EUS) users are significantly more effective at identifying multiple anatomic targets in a timed trial using the IR system [3]. Kinematics measurements, which record and analyse position, orientation, and motion of instruments, have been shown correlate well with the expertise of the user [2]. Experiments comparing LUS and EUS user performance with and without Image Registration (IR) show that the IR system can permit novice users to perform like experts in some tasks, and even appear to improve the performance of experts in some tasks [2]. Users preferred the Image Registration approach for both endoscopy and laparoscopy.

#### Materials and methods

Two volunteers were independently scanned in a GE Signa 3T MRI scanner. Each volunteer was instructed to lay down on the scanner table in four poses: supine, prone, left and right lateral decubitus. The volunteers were instructed to hold their breath while the acquisition was being performed. In all cases, the same pulse sequence was used: Axial, 2D, SPGR, Whole, Seq Minfull TE, 15 ms TR, 30 deg fa, 15.63 kHz, 40 cm FOV, 6 mm slice thickness, 46 slices in a  $256 \times 256$  matrix, 0.75 NEX, 10 locs.

The prone, right and left decubitus MRI datasets were independently registered to the corresponding supine scan. Before the registration was performed, the images were filtered using an anisotropic diffusion filter [4] to remove noise and improve the registration robustness. Rigid body image-based mutual information [5] was employed as registration method. The registration converged in all cases. 3D Slicer (version 2.6) was used to implement the image analysis pipeline as well as the visualization of the results.

**Table 1** Displacement for the organ and position

Subject 1												
Subject Pose	Positioning error with respect to supine pose (in mm)											
	Liver				Right Kidney				Left Kidney			
	Total	RL	AP	SI	Total	RL	AP	SI	Total	RL	AP	SI
Prone	6.62	5.91	2.65	1.33	5.71	0.56	4.67	3.24	12.24	0.31	4.10	11.53
Right decubitus	7.06	5.55	4.13	1.39	41.44	12.57	24.60	30.88	20.07	13.66	4.53	13.98
Left decubitus	6.97	5.94	3.09	1.94	19.36	8.51	10.79	13.64	33.57	25.04	5.57	21.65
Subject 2												
Subject Pose	Positioning error with respect to supine pose (in mm)											
	Liver				Right Kidney				Left Kidney			
	Total	RL	AP	SI	Total	RL	AP	SI	Total	RL	AP	SI
Prone	5.45	2.58	2.62	4.02	4.50	0.23	3.42	2.92	11.70	3.04	4.68	10.29
Right decubitus	9.45	4.08	1.69	8.35	9.62	2.62	8.46	3.76	12.42	6.31	7.97	7.14
Left decubitus	10.25	2.04	1.74	9.89	7.79	4.96	3.69	4.75	6.56	3.20	4.66	3.33

Three key abdominal structures were manually segmented by an expert using 3D Slicer, namely: liver, right kidney and left kidney. The segmentation was done in the original MRI scan space for each body pose before alignment. The registration results were double-checked by another expert to test for disparities. The segmentation were transformed to the supine scan space using the alignment matrices computed by the registration process.

Our figure of merit to assess organ displacement was the distance between the organ centroid (center of gravity) between supine (reference position) and the tested subject positions for each individual organ. The centroid provides a measurement of the overall total displacement. The distance between centroids was also analyzed along the main axes in the supine space: RL (left to right), AP (posterior to anterior) and SI (inferior to superior).

### Results

The alignment for Subject 1 is shown in Fig. 1. Subject 1 had additionally a CT image in supine position that is also shown. Table 1 shows the displacement for the organ and position. Prone is the pose with the least organ shift and the most consistent across subjects. The liver shows a modest displacement less than 1 cm for every pose. However, both kidneys show significant displacements with a range between 1 and 5 cm. Values for the comparison of prone and supine positions agree with the observations reported in previous studies [1].

### Discussion and conclusions

The shifts in abdominal organs with patient pose are significant, relative to instrument targeting requirements for image-guided procedures. While our initial hypothesis was that the liver was going to show a larger effect due to patient position, our results suggests that the kidneys are more prone to shift. This motion can be explain by the little constrains offered by the facial spaces surrounding the kidney. This result agrees with the conclusions presented in [1].

In summary, global information from a supine CT should likely not be used for guiding interventions when the patient is lying on his side, unless corrections are made for these gravity-induced effects. It appears from this very limited study that the degrees of organ motion will be highly dependent on the individual patient; likely due to factors such as patient age, sex, and degree of obesity. The scale of organ motion effects and the limitations of current body models (and the practical inability to perform multi-position scanning in the clinical setting) imply that successful image guided interventions will require accurate local real time images to support navigation to clinical targets.

### References

- [1] W. S. Ball, J. D. Wicks, F. A. Mettler, Jr. Prone-supine change in organ position: CT demonstration. *AJR*, 135:815–820, 1980.
- [2] G. Vosburgh, N. Stylopoulos, R. San José Estépar, R. E. Ellis, E. Samset, and C. C. Thompson. Eus and ct improve efficiency and structure identification over conventional EUS. *Endoscopy*, 65(6):866–870, 2007.
- [3] R. San José Estépar, Nicholas Stylopoulos, Randy Ellis, Eigil Samset, Carl-Fredrik Westin, Christopher Thompson, and Kirby Vosburgh. Towards scarless surgery: An endoscopic ultrasound navigation system for transgastric access procedures. *Aided Surgery*, 12(6):311–324, November 2007.
- [4] Karl Krissian, Flux-Based Anisotropic Diffusion Applied to Enhancement of 3-D Angiogram. *IEEE Trans. Med. Imaging* 21(11): 1440–1442 (2002).
- [5] P. Viola and W. M. Wells III, “Alignment by maximization mutual information,” in *Conference on Computer Vision*, E. Grimson, S. Shafer, A. Blake, and K. Sugihara, Eds. 1995, pp. 16–23, IEEE Computer Society Press, Los Alamitos, CA.

### Laser endoscope with variable target points for fetal surgery

Yamanaka N.<sup>1</sup>, Yamashita H.<sup>1</sup>, Liao H.<sup>2</sup>, Masamune K.<sup>1</sup>, Chiba T.<sup>3</sup>, Dohi T.<sup>1</sup>

<sup>1</sup>The University of Tokyo, Graduate School of Information Science and Technology, Tokyo, Japan

<sup>2</sup>The University of Tokyo, Graduate School of Engineering, Tokyo, Japan

<sup>3</sup>National Center for Child Health and Development, Clinical Research & Development, Tokyo, Japan

**Keywords** Laser coagulation · TTTS · Rigid endoscope · Coaxial irradiation · Controlling focal point

### Introduction

In fetal diseases, twin-to-twin transfusion syndrome (TTTS) is a target of fetal surgery. TTTS occurs in monochorionic twins due to the anastomosing vessels of the placenta. As a treatment of TTTS, fetoscopic laser photocoagulation of the vessels shows good outcomes. However, it has a risk of injuring the placenta with the tip of laser fiber while a surgeon focuses a laser beam on the targets. It is hard to navigate a set of a fetoscope and a laser fiber because the vessels move with the breath of mother. In order to make the surgery safer, we suggest an endoscope which can change the focal point of a laser beam without moving the endoscope itself.

### Materials and methods

The rigid-type endoscope, composed of relay lenses, transmits a laser beam coaxially (Fig. 1).

Each lens of the endoscope has a multi-coating of dielectric material for better transmission of visible and near infrared light of Nd:YAG or diode laser beam.

For coaxial irradiation, a hot mirror which reflects the near infrared light and transmits visible light is set between the endoscope and a camera. At first, the beam and guide light are reflected by the galvano mirrors towards the hot mirror, which further directs this beam into the endoscope. The usage of mirrors makes it possible to control the direction of the beam from the tip of the endoscope and change the position of focal spot. The galvano mirrors and camera are placed at optically symmetric point with respect to the hot mirror to ensure a large range of the irradiation angle.

We developed a prototype of the endoscope and its control unit (Fig. 2). The rigid endoscope, 7 mm in diameter, is consisted of objective lenses, relay lenses and eye lenses as that of a general endoscope. It has about 70 degrees viewing angle with an effective length of about 150 mm. The laser source is a clinically used Nd:YAG laser (Standard-Lichtleiter E-4070-B, Dornier MedTech) with a laser fiber of 400  $\mu\text{m}$  core diameter. The tip of the laser fiber is cooled by circulating water.

### Results and discussions

We observed a placental model by the endoscope and confirmed the performance of angular variations of laser beam using a guide light (diode laser,  $\lambda = 633 \text{ nm}$ ). The range of the irradiation angle was about  $-20$  to  $20$  degrees, a total of  $40$  degrees. The image had some blurring because of chromatic aberration, but it served the purpose of

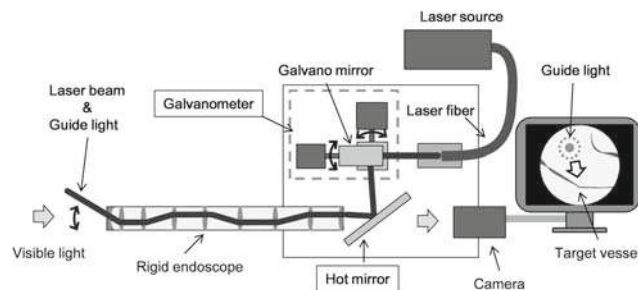


**Fig. 1** Concept of an endoscope that transmits a laser beam to arbitrary points in the endoscopic view